RESEARCH OUTPUTS / RÉSULTATS DE RECHERCHE

Low kinetic energy oxygen ion irradiationof vertically aligned carbon nanotubes

Acosta, Selene ; Casanova-Cháfer, Juan; Sierra Castillo, Ayrton; Llobet, Eduard; Snyders, Rony; Colomer, Jean-François; Quintana, Mildred; Ewels, Chris. P.; Bittencourt, Carla

[Link to publication]

Low Kinetic Energy Oxygen Ion Irradiation of Vertically Aligned Carbon Nanotubes

Selene Acosta [1,2,*] **, Juan Casanova-Chafer** [3] **, Ayrton Sierra-Castillo** [4] **, Eduard Llobet** [3] **, Rony Snyders** [1] **, Jean-François Colomer** [4] **, Mildred Quintana** [2] **, Chris Ewels** [5] **and Carla Bittencourt** [1]

1   Chimie des Interactions Plasma–Surface (ChIPS), Research Institute for Materials Science and Engineering, Université de Mons, 7000 Mons, Belgium; rony.snyders@umons.ac.be (R.S.); Carla.BITTENCOURT@umons.ac.be (C.B.)
2   Centro de Investigación en Ciencias de la Salud y Biomedicina, Universidad Autónoma de San Luis Potosí., San Luis Potosí 78210, Mexico; mildred@ifisica.uaslp.mx
3   MINOS Group, Universitat Rovira i Virgili, 43007 Tarragona, Spain; juan.casanova@urv.cat (J.C.-C.); eduard.llobet@urv.cat (E.L.)
4   Research Group on Carbon Nanostructures (CARBONNAGe), University of Namur, 5000 Namur, Belgium; ayrton.sierracastillo@unamur.be (A.S.-C.); jean-francois.colomer@unamur.be (J.-F.C.)
5   Institut des Matèriaux Jean Rouxel (IMN), CNRS UMR6502, Université de Nantes, 44322 Nantes, France; chris.ewels@cnrs-imn.fr
*   Correspondence: Selene.ACOSTAMORALES@umons.ac.be; Tel.: +52-489-41-56-68

Abstract: Vertically aligned multiwalled carbon nanotubes (v-CNTs) were functionalized with oxygen groups using low kinetic energy oxygen ion irradiation. X-ray photoelectron spectroscopy (XPS) analysis indicates that oxygen ion irradiation produces three different types of oxygen functional groups at the CNTs surface: epoxide, carbonyl and carboxyl groups. The relative concentration of these groups depends on the parameters used for oxygen ion irradiation. Scanning electron microscopy (SEM) shows that the macroscopic structure and alignment of v-CNTS are not affected by the ion irradiation and transmission electron microscopy (TEM) proves tip functionalization of v-CNTs. We observed that in comparison to oxygen plasma treatment, oxygen ion irradiation shows higher functionalization efficiency and versatility. Ion irradiation leads to higher amount of oxygen grafting at the v-CNTs surface, besides different functional groups and their relative concentration can be tuned varying the irradiation parameters.

Keywords: ion irradiation; functionalization; carbon nanotubes

1. Introduction

Carbon nanotubes (CNTs) are nanostructured material with high technological importance owing to their unique chemical and electronic properties. They have been reported as good candidates to replace silicon in different electronic devices due to their higher carrier velocity, nanoscale structure and relative low-cost large scale production [1]. Nevertheless, their inert surface limits their use in several applications, such as biological and gas sensor devices [2–4]. To tackle this issue, the CNTs surface properties can be altered through changes of their surface chemistry by functionalization. It has been shown that CNTs functionalization with oxygen groups can enhance their surface chemical reactivity [5,6] and change their hydrophobicity improving their dispersion in aqueous media [7,8], property that is of vital importance for their integration in biological systems. Moreover, oxygen groups can act as active sites for further functionalization increasing their potential applications in a vast variety of fields, such as drug delivery, bio imaging, water purification and catalysis, among others [9].

Vuković et al. reported in 2010 [10] that amino functionalization of CNTs can be easily implemented by chemical modification of carboxyl groups in oxidized CNTs, engineering CNTs capable of removing Cd^{2+} from water solutions. Regarding electronic properties, oxygen groups grafted at the CNTs surface can convert metallic CNTs into semiconducting [11]. Barinov et al. [11] showed that even a very small oxygen amount could alter the electronic structure of CNTs without altering their morphology.

Functionalization of CNTs has been achieved via different techniques such as wet chemistry, surface plasma treatment and simultaneous functionalization during synthesis or ion irradiation [12–15]. In order to obtain an optimal tailoring of the CNTs chemical and electronic properties, the functionalization technique used must be fully controlled. In this context, low kinetic ion irradiation consists of irradiating a target with ions of low kinetic energy, these ions interact with the sample in two different ways, they can bond directly to the atoms in the target, mainly in the intrinsic defects, or crosswise the sample creating new defects that can be used by other ions to create new functional groups.

Ion irradiation can alter the structure and the chemical, electronic and magnetic properties of carbon materials [16]. Additionally, junctions among carbon nanotubes can be created, which may have application in the reinforcement of materials for construction among others [17]. The ion kinetic energy during ion irradiation is an important parameter for optimal functionalization. It is considered low kinetic energy ion irradiation if the ions have an energy range from 100 eV to a few keV, and high kinetic energy ion irradiation if the range is of several keV to MeV [17,18]. The degree of interaction of the ions with the sample also depends on the displacement threshold energy T_d of the sample, that is, the minimum energy required by an atom through the impact of an energetic particle to be ejected from its original position [16]. Only if the kinetic energy imparted by the ions is higher than the T_d of the irradiated material the atoms will be moved and defects created.

Unlike others functionalization techniques, low energy ion irradiation is a clean, efficient and site-selective post-growth technique that does not generate liquid waste and allows functionalizing with a precise ion dose control, adjusting the quantity and energy of ions arriving to the sample surface [19]. In addition, this technique offers the possibility of scaling up to produce large quantities of functionalized CNTs for commercial use. Furthermore, different parameters for ion irradiation can be varied reducing the creation of defects on the structure of nanomaterials. Depending on the kinetic energy and the ion mass, the ions can traverse the nanomaterial without interaction with the target, contrary to bulk materials where all ions will interact with the sample [20]. Besides, ion irradiation of graphitic networks is of high interest in nano-engineering due to their ability of structural reorganization after irradiation, like no other material; during the reorganization new bonds around the defects are created restructuring the lattice [21].

Low kinetic energy ion irradiation of CNTs has been described mainly in theoretical works [22–24] and the limited experimental works reported are mostly in boron and nitrogen ion irradiation [19,25,26]. In this work, vertically aligned multi-walled carbon nanotubes (v-CNTs) are functionalized with oxygen groups using low kinetic energy ion irradiation, we evaluate the influence of the ion kinetic energy and irradiation time in the resulting oxygen functionalization. Vertically aligned nanotubes with their unidirectional electron transport facilitate the transducer operation in sensors [27]. Besides, their vertical geometry avoids the use of wet chemistry preventing contamination of the CNTs walls during integration of the active layer in the transducer. The v-CNTs were synthetized by thermal catalytic chemical vapor deposition technique. The structure and alignment of v-CNTs was observed before and after ion irradiation using scanning electron microscopy and transmission electron microscopy. The chemical functionalization of v-CNTs was characterized using X-ray photoelectron spectroscopy and Raman spectroscopy.

2. Materials and Methods

Vertically aligned multi-walled carbon nanotubes (v-CNTs) were synthesized by thermal catalytic chemical vapor deposition technique using C_2H_4 as a carbon source [27]. A multilayer system composed of Si/Al/Fe was the catalyst. Si wafers were used as substrates. An Al thin film (30 nm) was

deposited on Si wafers and then, after its oxidation, a 1.5 nm Fe layer was deposited and heated to 300 °C for three hours to form nanoparticles, which are responsible for the CNTs growth. The Al and Fe layers were prepared by magnetron sputtering using a Quorum device. For the v-CNTs growth, the reactor was heated to 750 °C in atmospheric pressure under He flow (500 sccm). The catalyst was placed inside the reactor and H_2 flow (200 sccm) was introduced into the reactor for 20 min. After that, C_2H_4 flow (60 sccm) was introduced into the reactor for 24 min. After the growth, H_2 and C_2H_4 flows were switched off and a flow of He was used to clean the reactor (500 sccm). The outer diameter distribution of the v-CNTs obtained was 10–40 nm.

The low kinetic energy oxygen ion irradiation in v-CNTs was performed in a vacuum chamber system (PREVAC-541) using as an ion source a Tectra plasma source TPIS, where microwave energy is used to create gas plasma at the plasma cup from which ions are extracted. Microwaves with a frequency of 2.45 GHz were generated by a magnetron coupled to a coaxial feedthrough structure, which guided the microwaves into the plasma cup containing low pressure O_2 gas. The electrons generated in the plasma undergo cyclotron resonance motion increasing their perpendicular kinetic energy due to a magnetic quadrupole arranged around the discharge chamber. Subsequently, when the energized free electrons collide with the gas in the volume, they cause ionization of the gas if their kinetic energy is larger than the ionization energy of the atoms or molecules. The ion extraction optics was composed of two grids located at the open end of the plasma cup, a positive voltage was applied to the first grid to accelerate ions extracting them from the plasma out to the sample, the other grid had a negative voltage and assisted in the ion extraction and the beam current.

Oxygen ion irradiation was performed varying separately the irradiation time and the ion kinetic energy. For the samples functionalized with different irradiation time the ion kinetic energy was fixed at 1 keV and the time was varied from 1, 2.5, 5 and 10 min. The samples functionalized varying the ion kinetic energy had irradiation time fixed to 5 min, the different ion kinetic energies were 0.1, 0.25, 0.5, 1, 1.5 and 2 keV. For all samples the current induced by the ion irradiation energy was 10 μA, certifying that the number of ions reaching the samples were the same (Table 1).

Table 1. Summary of irradiation parameters used for oxygen functionalization of vertically aligned multiwalled carbon nanotubes (v-CNTs), oxygen (at. %) and carbon (at. %) relative concentration obtained by X-ray photoelectron spectroscopy (XPS).

| Irradiation Time (min)	Ion Kinetic Energy (keV)	Oxygen Content (at. %)	Carbon Content (at. %)
0	–	1.7	98.3
1	1	6.7	93.3
2.5	1	10.0	90.0
5	1	14.2	85.8
10	1	20.0	80.0
5	0	8.0	92.0
5	0.1	8.4	91.6
5	0.25	9.8	90.2
5	0.5	15.4	84.6
5	1.5	14.5	85.5
5	2	16.0	84.0

The vertical alignment and the morphology of v-CNTs were characterized before and after oxygen ion irradiation by scanning electron microscopy (SEM) using a JEOL-JSM-7500F-Field Emission Scanning Electron Microscope operated at 15 kV and transmission electron microscopy (TEM) using a JEM-1011 Jeol Ltd. Tokyo, Japan.

The chemical composition of the v-CNTs was studied with X-ray photoelectron spectroscopy (XPS) using a VERSAPROBE PHI 5000 from Physical Electronics, Chanhassen, MN U.S. equipped with a monochromatic Al Kα X-ray source. The XPS analysis chamber is connected to the ion irradiation vacuum chamber system to avoid contaminations. C1s and O1s core level spectra were recorded for each sample with an energy resolution of 0.6 eV.

Raman spectroscopy was collected using a Micro-Raman system (Senterra Bruker Optik GmbH, Ettlingen, Germany) with a resolution of 3 cm^{-1} using as excitation source a laser with a wavelength of 532 nm and 20 mW of power.

3. Results and Discussion

The macroscopic morphology and alignment of v-CNTs were evaluated with SEM microscopy before and after the oxygen ion irradiation in order to estimate if disorder was induced by ions impacting onto the sample surface. We observed that neither the density nor the alignment of CNTs were affected by the ion irradiation treatment (Figure 1).
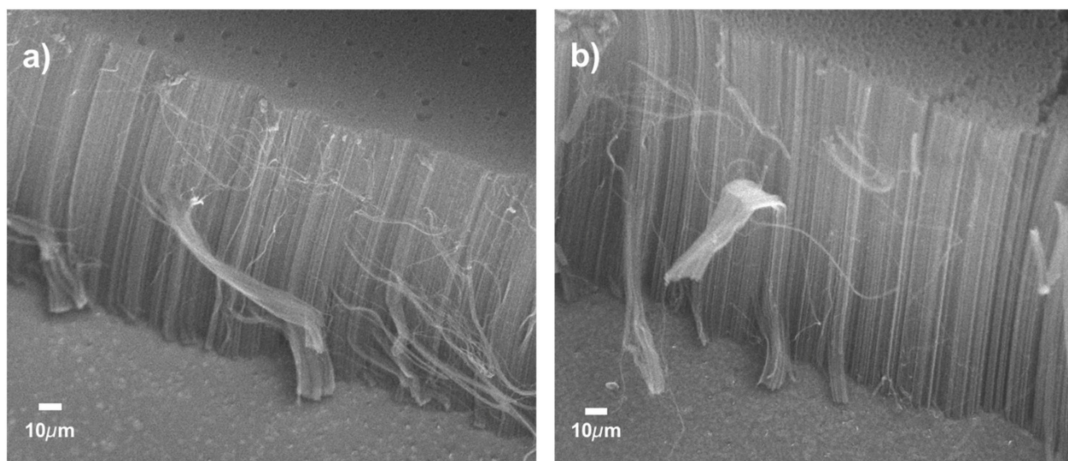

Figure 1. Cross section SEM images of v-CNTs before (**a**) and after 5 min of irradiation with oxygen ions with 1 keV of kinetic energy (**b**).

The understanding of the dependency of the oxygen bonding configurations in v-CNTs on the different parameters used during ion irradiation is a key step for optimal controlling functionalization and, consequently tailoring CNTs properties for applications such as in sensing. X-ray photoelectron spectroscopy (XPS) is a surface technique that, besides providing information on the relative atomic concentration of the elements present on a sample, is also suitable to characterize changes in the bonding configuration of the atoms via the chemical shift, i.e., via the analysis of the shift in the binding energy of the core electrons of the different atoms composing a sample.

We first recorded XPS survey spectra to evaluate if the oxygen ion irradiation had grafted undesired elements other than oxygen at the CNT surface. Figure 2 shows typical survey spectra recorded on v-CNTs before and after 5 min of irradiation with oxygen ions with 1 keV of kinetic energy. We could observe in the spectrum recorded before the ion irradiation a high intensity peak centered at 284.4 eV, generated by photoelectrons emitted from the C1s electronic level, and a very low intensity peak at 532.6 eV associated to oxygen contamination during the v-CNTs synthesis, evaluated to be 1.7 at. %. After ion irradiation the relative intensity of the peak generated by C1s photoelectrons decreased and the intensity of the peak at 532.6 eV corresponding to O1s photoelectrons increased remarkably. No other elements were found in the samples.
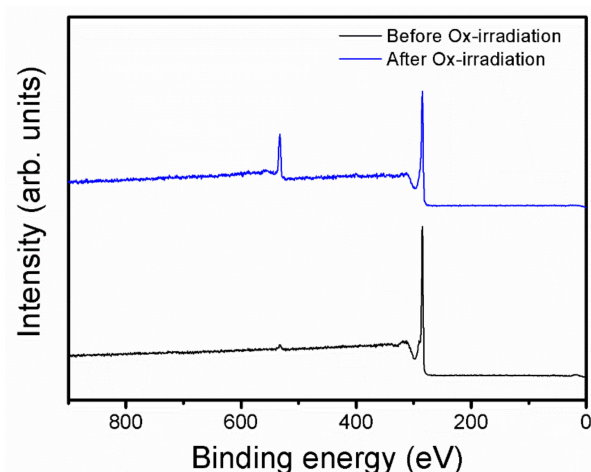
Figure 2. XPS survey spectra comparison between v-CNTs before (black line) and after 5 min of irradiation with oxygen ions with 1 keV of kinetic energy (blue line).

Figure 3 summarizes the change in the relative oxygen concentration when v-CNTs were irradiated with oxygen ions with different kinetic energies and irradiation times. Increasing the irradiation time (1, 2.5, 5 and 10 min) the relative concentration of oxygen increased from 1.7 to 20.0 at. % (Figure 3a). For a fixed irradiation time (5 min) we could divide the resulting amount of oxygen ion grafting in two regimes (Figure 3b): from 0.5 to 2 keV, the relative oxygen concentration remained almost constant (15.0 at. %) independent of the ion energy. As the number of oxygen ions arriving at the sample surface was fixed throughout the experiment, we could conclude that the ion kinetic energy in this range did not affect the rate of ions grafted at the CNT surface. The amount of oxygen ions implanted thus depended only on the treatment time. The second regime was observed for oxygen ion irradiation from 0 up to 0.5 keV (Figure 3b), it is clear that when CNTs were irradiated with ions with 0 keV kinetic energy, i.e., the grid supply at the extractor was set to 0 keV, the amount of oxygen grafted was lower. Under these conditions no specific ion kinetic energy was selected, and all types of species generated inside the plasma chamber were able to reach the sample surface, including neutrals species. It is important to mention that the distance between the exit of the plasma cup in the Tectra ion source and the surface of the sample was about 12 cm, thus it was a remote plasma treatment in which the species with short-life time recombine before reaching the sample surface [28]. Under these conditions instead of ion irradiation, functionalization occurred via a plasma treatment. The quantity of oxygen grafted during this remote oxygen plasma treatment was 8.0 at. % about half that produced by ion energy irradiation, with ion kinetic energies from 0.5 to 2 keV (Figure 3b). The increase in the grafting of oxygen for increasing ion kinetic energy could be associated to an increase in the probability of defect creation as discussed by Lehtinen et al. in 2010 [29]. These authors, using atomistic computer simulations based on analytical potential and density-functional theory models, showed that for carbon nanostructures the probability of defect creation during low-mass ion irradiation, had a sharp increase up to 0.5 keV kinetic energy followed by a gradual decrease. This shows that the functionalization efficiency using low kinetic energy ion irradiation was higher than in the remote plasma treatment, since the impacting oxygen species were more energetic increasing the probability of creating defect sites into the CNT lattice [30]. Additionally, the oxygen species shorter lifetimes increased the possibility for recombination into stable gas-phase species unlikely to react with the tubes.
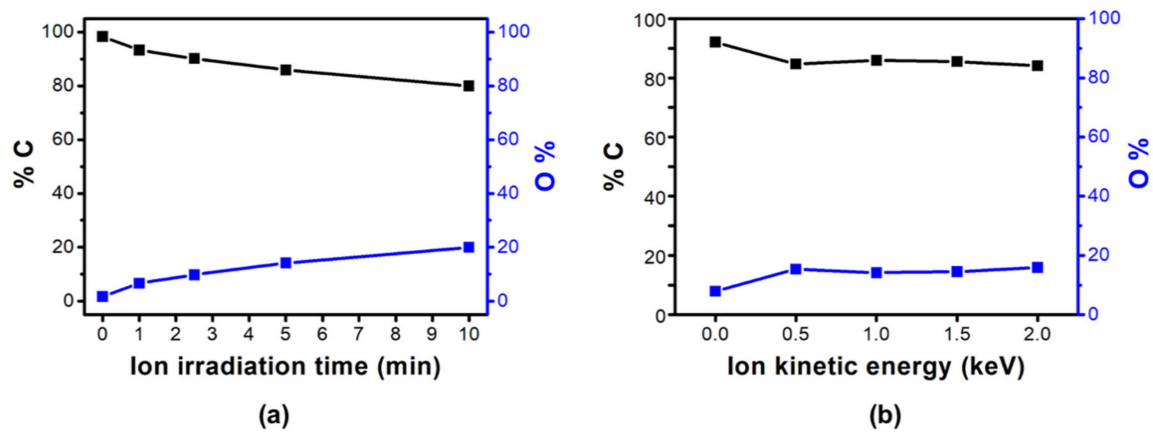
Figure 3. Carbon and oxygen content in v-CNTs before and after oxygen functionalization in function of ion irradiation time (**a**) and ion kinetic energy (for a fixed time: 5 min) (**b**). When the ion irradiation time is zero it corresponds to v-CNTs pristine. For ion energy equal to 0 keV the oxidation occurs through a remote plasma treatment rather than to an ion-implantation process.

A detailed analysis of the C1s XPS spectrum gives information on the chemical configuration of the oxygen grafted in the graphitic network. Figure 4 shows a comparison between the C1s spectra recorded on the pristine v-CNTs and after 10 min of oxygen ion irradiation at 1 keV of ion kinetic energy and the result of the curve fitting reproducing each spectrum.
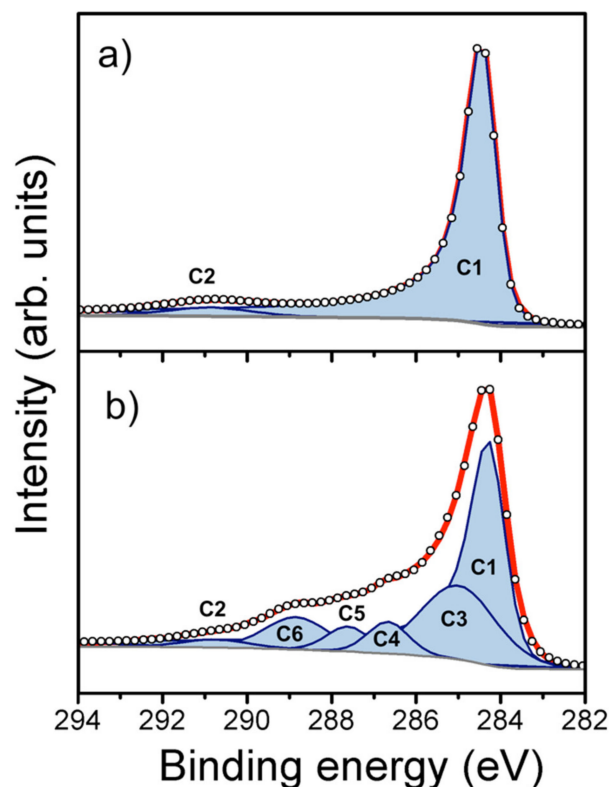
Figure 4. XPS analysis of v-CNTs pristine (**a**) and v-CNTs after 10 min of irradiation with oxygen ions with ion kinetic energy of 1 keV (**b**). C1 is assigned to sp^2-C (284.4 eV), C2 to π-plasmon excitations (290.9 eV), C3 to sp^3-C (285.0 eV), C4 to epoxide groups C–O–C (286.6 eV), C5 to carbonyl groups C=O (287.5 eV) and C6 to carboxyl groups –COOH (288.8 eV). Components peaks result from a least-squares fitting procedure.

The pristine C1s spectrum is asymmetric, due to a re-adjustment of the Fermi level caused by electron-hole interaction after the electron scattering. In order to reproduce this asymmetry, the fitting of C1s peak was made with the Doniach–Sunjic function [31]. The peak had a binding energy of 284.4 eV and was reported to be generated by photoelectrons emitted from sp^2 carbon atoms [11]. We also observed a low intensity broad peak centered at 290.9 eV, corresponding to photoelectrons that lose kinetic energy to π-plasmon excitations. To reproduce this peak a Gaussian–Lorentzian was used (Figure 4a).

The C1s XPS spectra recorded after v-CNTs irradiation with oxygen ions show a drastic change, widening in the range 285–290 eV, due to the bonding of oxygen to carbon atoms (Figure 4b, supplementary). To reproduce the spectrum for the sample irradiated 10 min it was necessary to use six components, the two used in the fitting of pristine v-CNTs and four other symmetric peaks (Gaussian–Lorentzian). These components were centered at binding energies of 285.0 eV, 286.6 eV, 287.5 eV and 288.8 eV.

The component at 285.0 eV was assigned to sp^3 carbon bonding occurring at defects introduced in the carbon lattice by ion irradiation. This could include interlayer and intertube cross-linking defects, amorphization and carbon bonding to CO_x species. Induced in a controllable way, these defects can cause beneficial changes in chemical and electronic properties of the CNTs, promoting their application in different fields [16]. The components at 286.6 eV, 287.5 eV and 288.8 eV were associated to carbon bonded to oxygen. The electronegative oxygen atoms induce a positive charge in the carbon atoms thus changing the electron screening of their nucleus. This increased consequently the binding energy of the electrons, explaining the shift to higher binding energies for the components in the C1s spectra. Using spin polarized density functional calculations within the local density approximation (LDA) for the interpretation of the C1s XPS peak of oxygen functionalized carbon nanotubes, Bittencourt et al. [12], assigned the component at 286.6 eV to epoxide groups (C–O–C), the component 287.5 eV to carbonyl groups (C=O) and 288.8 eV to carboxyl groups (–COOH).

In order to understand the effect of varying the ion irradiation parameters in the chemistry of the v-CNTs, we analyzed the C1s XPS spectrum of each sample (Table 2, Table S1, Figures S1–S7). To corroborate our results, the analysis of O1s XPS spectra was also performed (Table S2, Figures S8–S17). The same number of C–O components were obtained in C1s and O1s analysis.

Table 2. Relative area (%A) of the components used the reproduce the C1s peak. The binding energy assignments were reported by Bittencourt et al. 2011.

Irradiation Time (min)	Ion Kinetic Energy (keV)	sp^2-C (%A) C1 284.4 eV	sp^3-C (%A) C3 285.0 eV	C–O–C (%A) C4 286.6 eV	C=O (%A) C5 287.5 eV	–COOH (%A) C6 288.8 eV	Plasmon (%A) C2 290.9 eV
0	–	96.3	0	0	0	0	3.7
1	1	86.2	9.0	0.7	1.9	0	2.2
2.5	1	83.0	11.5	1.7	2.4	0	1.4
5	1	71.7	16.8	3.1	4.7	2.9	0.8
10	1	62.7	20.0	4.5	3.8	7.2	1.9
5	0	85.2	8.8	5.5	0	0	0.5
5	0.1	92.9	5.5	1.3	0	0.3	0
5	0.25	84.2	9.8	2.6	0	1.9	1.5
5	0.5	71.2	15.7	3.3	2	5.7	2.1
5	1.5	69.7	19.0	4.2	2.4	3.7	1.1
5	2	72.0	15.5	3.9	4.2	2.7	1.7

Figure 5 shows the variation in the relative area of each component used to reproduce the C1s peak as a function of the treatment time and the ion kinetic energy. The relative contribution of component C1 (graphitic carbon (sp^2-C)) decreased from the 96.3% in pristine v-CNTs to 62.7% when the treatment time reached 10 min, indicating that the oxygen functionalization occurred through breakdown of π bonding in the sp^2-C bond. The relative area of component C2 (sp^3-C) increased to 20% after 10 min of treatment (Figure 5a).
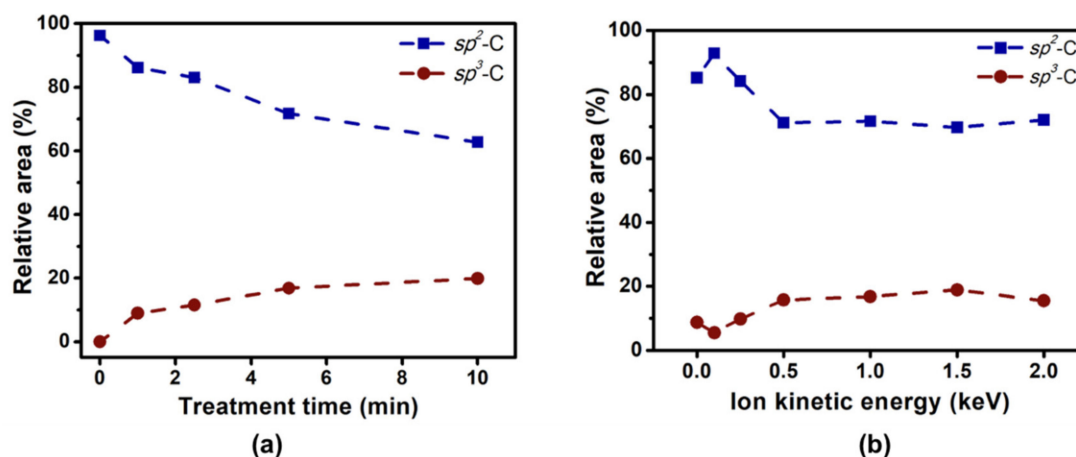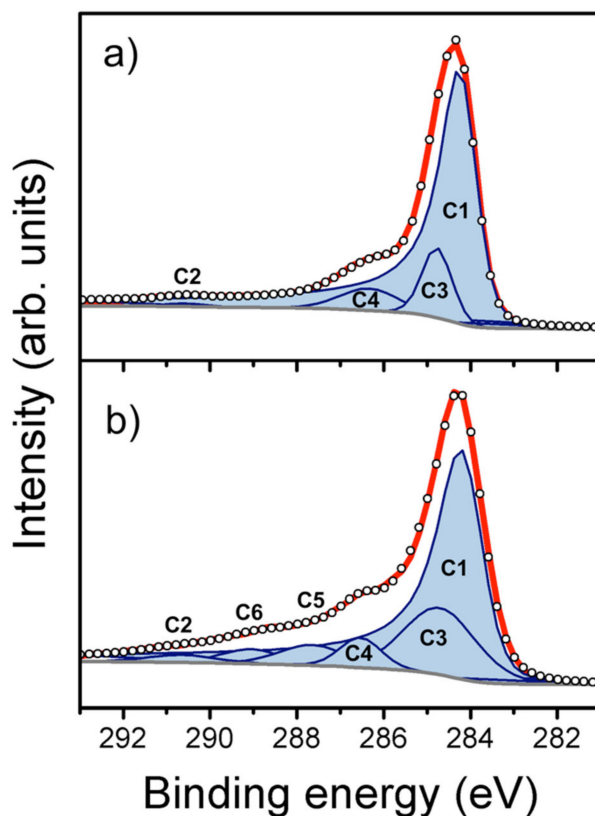
Figure 5. Variation in relative area of the components of carbon sp^2-C (C1) and carbon sp^3-C (C3) used to reproduce the C1s XPS spectrum of v-CNTs as a function of the treatment time (ion kinetic energy 1 keV; (**a**)) and the ion kinetic energy (fixed treatment time: 5 min; (**b**)).

When the treatment time was fixed to 5 min and the ion kinetic energy was the variant parameter, we observed that the ion energy did not significantly affect the relative area of the graphitic carbon component (C1), remaining in a range from 69.7% to 72.0% (for the range of energies from 0.5 to 2 keV). Similarly, the area of the component C2 (sp^3-C) remained in a range from 15.7% to 19.0%.

These results suggest that for the samples irradiated with ion kinetic energy varying from 0.5 to 2 keV, approximately the same number of ions interact with the carbon nanotubes. At 0 keV kinetic energy (a remote plasma treatment [32]), only 8.8% of the sp^2 carbon (C1) was transformed into sp^3 (C3) and 5.5% into oxygen-bound carbon species (C4), confirming that the remote plasma treatment generated less defects at the CNT surface than ion irradiation (Figure 5b), with much lower oxygen grafting at the CNT surface (Figure 3b).

It is interesting to compare the grafting of oxygen atoms for 0 keV (remote plasma functionalization) with the ion irradiation results (Figures 6 and 7b). In the case of remote plasma functionalization, the only C–O bonding observed comes from epoxide groups. These consist of single oxygen atoms bonded covalently to a sp^2-C surface, forming covalent bonds with two carbon neighbors with the oxygen atom sitting above the C–C bond centre. This is the least disruptive oxygen functional group (indeed epoxide groups can be added to graphene simple trough ozone exposure with UV light [33]), since they do not require carbon dangling bonds, and hence associated hole or edge formation. This therefore confirmed that the remote plasma was only adding very low energy isolated oxygen atoms to the nanotube surface (probably primarily neutrals) with minimal damage and disruption of the carbon layers. Epoxide oxygen could also be removed through relatively gentle reducing processes.

In contrast, the ion-implantation results show high concentrations of carbonyl and carboxyl groups, demonstrating that the lattice was being disrupted and carbon dangling bonds created, which were being oxygenated. This was consistent with a picture where incoming charged oxygen ions were arriving with kinetic energies far above the knock-on threshold energies of the lattice carbon, resulting in carbon displacements and increased local damage. This was also visible in the production of sp^3-C carbon atoms as collateral damage. Thus the two processes were complementary, allowing choice of oxygen chemical functional group addition depending on end-application requirements.

Figure 6. XPS analysis of v-CNTs functionalized by plasma treatment (0 keV of ion kinetic energy) (**a**) and by ion irradiation with 2 keV of ion kinetic energy (**b**). The treatment time was 5 min for the two samples. C1 is assigned to sp^2-C (284.4 eV), C2 to π-plasmon excitations (290.9 eV), C3 to sp^3-C (285.0 eV), C4 to epoxide groups C–O–C (286.6 eV), C5 to carbonyl groups C=O (287.5 eV) and C6 to carboxyl groups –COOH (288.8 eV). Components peaks result from a least-squares fitting procedure.
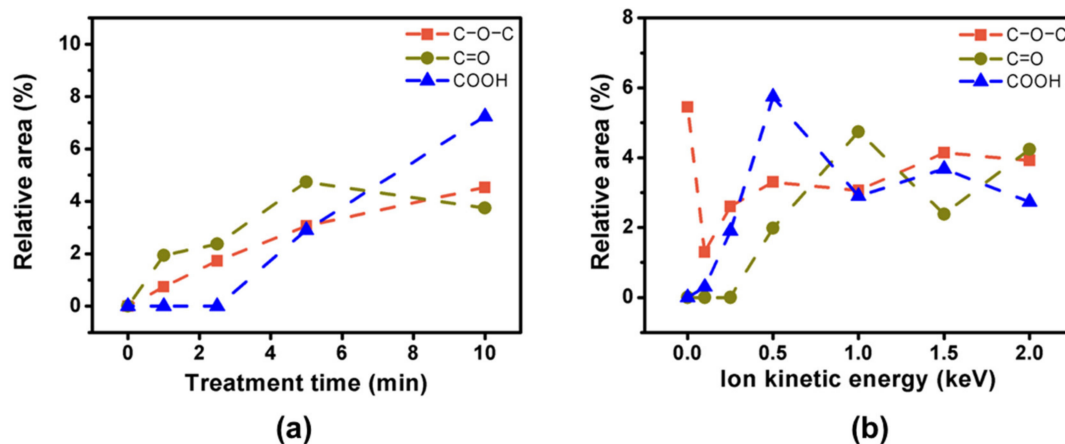
Figure 7. Variation in relative area of the components of carbon bonded to oxygen (C4 (C–O–C), C5 (C=O) and C6 (–COOH)) used to reproduce the C1s XPS spectrum of v-CNTs as a function of the treatment time (ion energy 1 keV; (**a**)) and the ion kinetic energy (treatment time 5 min; (**b**)).

We could further understand the oxidation processes occurring during ion irradiation by exploring the change in relative concentration of different C–O species over time (Figure 7a). Just as for the plasma treatment, epoxide species start forming on the basal plane from the beginning of the treatment, and gradually increase in concentration over the time. In parallel there was an extremely initial rapid formation of carbonyl groups. This presumably involved functionalization of tube tips, which are much more chemically reactive than the tube sidewalls and represent preferential addition sites [34]. During

this period there was a gradual increase in sp^3-C indicating the ion irradiation process is beginning to damage the nanotube carbon network (Figure 5a). After 5 min the network was sufficiently damaged that holes and internal edges are formed. These were C=O and –COOH edge-terminated, giving rise to a corresponding increase in the C=O and –COOH C1s peaks in the XPS.

The carbonyl groups were intermediate states and could oxygen saturate, transforming to carboxyl groups, helping to explain the relative stability in carbonyl concentration and large increase in –COOH in the C1s peak from 5 to 10 min. This process would be kinetically dependent on the rate of damage site and hole formation (i.e., new dangling bond creation rate), and was also reflected in the ion energy study (Figure 7b). As the ion kinetic energy increased there was a steady decrease in epoxide concentration, primarily because at higher energies there is an increased chance of damaging the lattice and so inserting oxygen as other (carbonyl or carboxyl) forms. The slight decrease in the sp^3-C component observed when the sample was irradiated with 0.1 keV ions could be associated to a preferential removal of physically adsorbed species (amorphous carbon and oxygen species including water) occurring during the synthesis and due to the exposure to ambient air.

Raman spectroscopy data shows variations in the ratio of relative intensity of the primary G- and D-peaks consistent with the interpretation we present here based on the XPS data, i.e., there was a general trend of increasing D to G-peak intensity ratio with both ion treatment time and energy consistent with an overall increase in disorder in the structure (see 343 Supplementary Figure S18 and associated supplementary discussion).

Figure 8 shows the typical TEM images recorded on carbon nanotubes pristine (Figure 8a) and carbon nanotubes irradiated for 5 min with oxygen ions with kinetic energy of 2 keV (Figure 8b) samples. The pristine nanotubes show a certain degree of disorder, typical of chemical vapor deposition (CVD) grown non-annealed multi-walled CNTs. The overall structure of CNTs was maintained after oxygen ion irradiation with no significant degradation such as amorphization and formation of amorphous carbon aggregates. However, high resolution TEM microscopy would be needed to expand the analysis of the creation of smaller defects such as vacancies, vacancy-aggregates and interlayer defects. While the pristine CNTs had closed tips, after oxygen ion irradiation the tips could be seen to be now open, evidence of oxygen tip attack and functionalization.
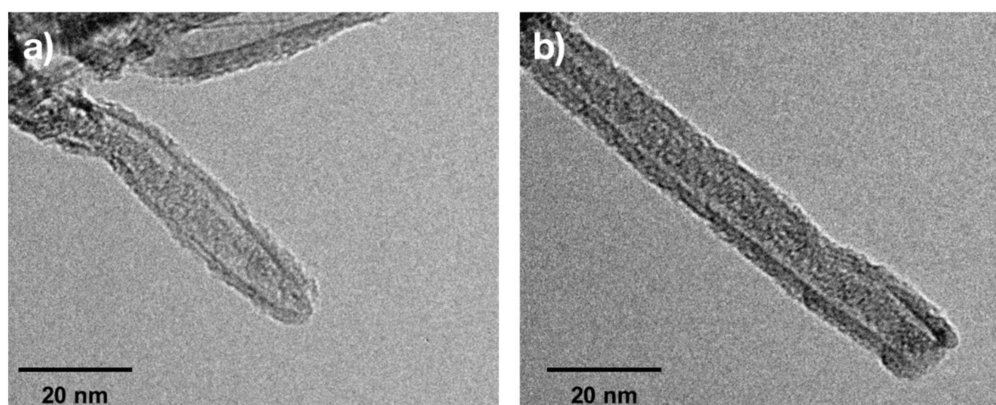
Figure 8. TEM microscopy of carbon nanotubes pristine (**a**) and carbon nanotubes irradiated for 5 min with oxygen ions with kinetic energy of 2 keV (**b**).

4. Conclusions

Different oxygen functional groups can be created at the surface of vertically aligned carbon nanotubes by low kinetic energy oxygen ion irradiation. We show that defect creation, the chemical nature and concentration of functional groups depended on the irradiation time and the ion kinetic energy, indicating that low kinetic energy ion irradiation was an optimal functionalization method that could be used to fine tune the type and concentration of functional groups grafted at the carbon nanotube surface. The versatility of the method was a very clear advantage in comparison to other

functionalization techniques, because using low kinetic ion irradiation we could tailor the surface reactivity of carbon nanotubes specifically for different applications, in a clean way and employing very short treatment times.

Conflicts of Interest: The authors declare no conflict of interest.

References

1. Li, W.Z.; Xie, S.S.; Qian, L.X.; Chang, B.H.; Zou, B.S.; Zhou, W.Y.; Zhao, R.A.; Wang, G. Large-scale synthesis of aligned carbon nanotubes. *Science* **1996**, *274*, 1701–1703. [CrossRef] [PubMed]

2. Fam, D.W.H.; Palaniappan, A.; Tok, A.I.Y.; Liedberg, B.; Moochhala, S.M. A review on technological aspects influencing commercialization of carbon nanotube sensors. *Sens. Actuators B Chem.* **2011**, *157*, 1–7. [CrossRef]

3. Bondavalli, P.; Legagneux, P.; Pribat, D. Carbon nanotubes based transistors as gas sensors: State of the art and critical review. *Sens. Actuators B Chem.* **2009**, *140*, 304–318. [CrossRef]

4. Vardharajula, S.; Ali, S.Z.; Tiwari, P.M.; Eroğlu, E.; Vig, K.; Dennis, V.A.; Singh, S.R. Functionalized carbon nanotubes: Biomedical applications. *Int. J. Nanomed.* **2012**, *7*, 5361. [CrossRef]

5. Yoo, K.P.; Kwon, K.H.; Min, N.K.; Lee, M.J.; Lee, C.J. Effects of O2 plasma treatment on NH3 sensing characteristics of multiwall carbon nanotube/polyaniline composite films. *Sens. Actuators B Chem.* **2009**, *143*, 333–340. [CrossRef]

6. Malik, R.; McConnell, C.; Alvarez, N.T.; Haase, M.; Gbordzoe, S.; Shanov, V. Rapid, in situ plasma functionalization of carbon nanotubes for improved CNT/epoxy composites. *RSC Adv.* **2016**, *6*, 108840–108850. [CrossRef]

7. Lobo, A.O.; Ramos, S.C.; Antunes, E.F.; Marciano, F.R.; Trava-Airoldi, V.J.; Corat, E.J. Fast functionalization of vertically aligned multiwalled carbon nanotubes using oxygen plasma. *Mater. Lett.* **2012**, *70*, 89–93. [CrossRef]

8. Trulli, M.G.; Sardella, E.; Palumbo, F.; Palazzo, G.; Giannossa, L.C.; Mangone, A.; Comparelli, R.; Musso, S.; Favia, P. Towards highly stable aqueous dispersions of multi-walled carbon nanotubes: The effect of oxygen plasma functionalization. *J. Colloid Interface Sci.* **2017**, *491*, 255–264. [CrossRef]

9. Muhulet, A.; Miculescu, F.; Voicu, S.I.; Schütt, F.; Thakur, V.K.; Mishra, Y.K. Fundamentals and scopes of doped carbon nanotubes towards energy and biosensing applications. *Mater. Today Energy* **2018**, *9*, 154–186. [CrossRef]

10. Vuković, G.D.; Marinković, A.D.; Čolić, M.; Ristić, M.Đ.; Aleksić, R.; Perić-Grujić, A.A.; Uskoković, P.S. Removal of cadmium from aqueous solutions by oxidized and ethylenediamine-functionalized multi-walled carbon nanotubes. *Chem. Eng. J.* **2010**, *157*, 238–248. [CrossRef]

11. Barinov, A.; Gregoratti, L.; Dudin, P.; La Rosa, S.; Kiskinova, M. Imaging and spectroscopy of multiwalled carbon nanotubes during oxidation: Defects and oxygen bonding. *Adv. Mater.* **2009**, *21*, 1916–1920. [CrossRef]

12. Bittencourt, C.; Navio, C.; Nicolay, A.; Ruelle, B.; Godfroid, T.; Snyders, R.; Colomer, J.-F.; Lagos, M.J.; Ke, X.; Van Tendeloo, G.; et al. Atomic oxygen functionalization of vertically aligned carbon nanotubes. *J. Phys. Chem. C* **2011**, *115*, 20412–20418. [CrossRef]

13. Datsyuk, V.; Kalyva, M.; Papagelis, K.; Parthenios, J.; Tasis, D.; Siokou, A.; Kallitsis, I.; Galiotis, C. Chemical oxidation of multiwalled carbon nanotubes. *Carbon* **2008**, *46*, 833–840. [CrossRef]

14. Korusenko, P.M.; Nesov, S.N.; Povoroznyuk, S.N.; Bolotov, V.V.; Knyazev, E.V. Functionalization of multi-walled carbon nanotubes using ion beams of various intensities. *AIP Conf. Proc.* **2018**, *2007*, 040008. [CrossRef]

15. Xia, W.; Schlüter, O.F.K.; Liang, C.; van den Berg, M.W.; Guraya, M.; Muhler, M. The synthesis of structured Pd/C hydrogenation catalysts by the chemical vapor deposition of Pd (allyl) Cp onto functionalized carbon nanotubes anchored to vapor grown carbon microfibers. *Catal. Today* **2005**, *102*, 34–39. [CrossRef]

16. Krasheninnikov, A.V.; Banhart, F.J.N.M. Engineering of nanostructured carbon materials with electron or ion beams. *Nat. Mater.* **2007**, *6*, 723. [CrossRef]

17. Krasheninnikov, A.V.; Nordlund, K. Irradiation effects in carbon nanotubes. *Nucl. Instrum. Methods Physics Res. Sect. B Beam Interact. Mater. Atoms* **2004**, *216*, 355–366. [CrossRef]

18. Kamimura, T.; Yamamoto, K.; Kawai, T.; Matsumoto, K. N-type doping for single-walled carbon nanotubes by oxygen ion implantation with 25 eV ultralow-energy ion beam. *Jpn. J. Appl. Phys.* **2005**, *44*, 8237. [CrossRef]

19. Bangert, U.; Bleloch, A.; Gass, M.H.; Seepujak, A.; Van den Berg, J. Doping of few-layered graphene and carbon nanotubes using ion irradiation. *Phys. Rev. B* **2010**, *81*, 245423. [CrossRef]

20. Krasheninnikov, A.V.; Nordlund, K. Ion and electron irradiation-induced effects in nanostructured materials. *J. Appl. Phys.* **2010**, *107*, 3. [CrossRef]

21. Krasheninnikov, A.V.; Nordlund, K.; Keinonen, J. Production of defects in supported carbon nanotubes under ion irradiation. *Phys. Rev. B* **2002**, *65*, 165423. [CrossRef]

22. Shemukhin, A.A.; Stepanov, A.V.; Nazarov, A.V.; Balakshin, Y.V. Simulation of defects formation in nanotubes under ion irradiation. *Nucl. Instrum. Methods Phys. Res. Sect. B Beam Interact. Mater. Atoms* **2019**. [CrossRef]

23. Krasheninnikov, A.V.; Nordlund, K.; Sirviö, M.; Salonen, E.; Keinonen, J. Formation of ion-irradiation-induced atomic-scale defects on walls of carbon nanotubes. *Phys. Rev. B* **2001**, *63*, 245405. [CrossRef]

24. Salonen, E.; Krasheninnikov, A.V.; Nordlund, K. Ion-irradiation-induced defects in bundles of carbon nanotubes. *Nucl. Instrum. Methods Phys. Res. Sect. B Beam Interact. Mater. Atoms* **2002**, *193*, 603–608. [CrossRef]

25. Scardamaglia, M.; Struzzi, C.; Rebollo, F.J.A.; De Marco, P.; Mudimela, P.R.; Colomer, J.F.; Amati, M.; Gregoratti, L.; Petaccia, L.; Snyders, R. Tuning electronic properties of carbon nanotubes by nitrogen grafting: Chemistry and chemical stability. *Carbon* **2015**, *83*, 118–127. [CrossRef]

26. Xu, F.; Minniti, M.; Giallombardo, C.; Cupolillo, A.; Barone, P.; Oliva, A.; Papagno, L. Nitrogen ion implantation in single wall carbon nanotubes. *Surface Sci.* **2007**, *601*, 2819–2822. [CrossRef]

27. Colomer, J.F.; Ruelle, B.; Moreau, N.; Lucas, S.; Snyders, R.; Godfroid, T.; Navio, C.; Bittencourt, C. Vertically aligned carbon nanotubes: Synthesis and atomic oxygen functionalization. *Surface Coat. Technol.* **2011**, *205*, S592–S596. [CrossRef]

28. Ruelle, B.; Felten, A.; Ghijsen, J.; Drube, W.; Johnson, R.L.; Liang, D.; Erni, R.; Van Tendeloo, G.; Peeterbroeck, S.; Dubois, P.; et al. Functionalization of MWCNTs with atomic nitrogen. *Micron* **2009**, *40*, 85–88. [CrossRef]

29. Lehtinen, O.; Kotakoski, J.; Krasheninnikov, A.V.; Tolvanen, A.; Nordlund, K.; Keinonen, J. Effects of ion bombardment on a two-dimensional target: Atomistic simulations of graphene irradiation. *Phys. Rev. B* **2010**, *81*, 153401. [CrossRef]

30. Tessonnier, J.P.; Villa, A.; Majoulet, O.; Su, D.S.; Schlögl, R. Defect-mediated functionalization of carbon nanotubes as a route to design single-site basic heterogeneous catalysts for biomass conversion. *Angew. Chem. Int. Ed.* **2009**, *48*, 6543–6546. [CrossRef]

31. Doniach, S.; Sunjic, M. Many-electron singularity in X-ray photoemission and X-ray line spectra from metals. *J. Phys. C Solid State Phys.* **1970**, *3*, 285. [CrossRef]

32. Zhu, H.; Qin, X.; Cheng, L.; Azcatl, A.; Kim, J.; Wallace, R.M. Remote plasma oxidation and atomic layer etching of MoS2. *ACS Appl. Mater. Interfaces* **2016**, *8*, 19119–19126. [CrossRef] [PubMed]

33. GÜNEŞ, F.; Han, G.H.; Shin, H.J.; Lee, S.Y.; Jin, M.; Duong, D.L.; Chae, S.J.; Kim, E.S.; Yao, F.; Benayad, A.; et al. UV-light-assisted oxidative sp3 hybridization of graphene. *Nano* **2011**, *6*, 409–418. [CrossRef]

34. Scardamaglia, M.; Amati, M.; Llorente, B.; Mudimela, P.; Colomer, J.F.; Ghijsen, J.; Ewels, C.; Snyders, R.; Gregoratti, L.; Bittencourt, C. Nitrogen ion casting on vertically aligned carbon nanotubes: Tip and sidewall chemical modification. *Carbon* **2014**, *77*, 319–328. [CrossRef]